Light Measurement using the Photometrics-PXL1300L CCD Camera

Sumanta N. Pattanaik[1] and Kenneth E. Torrance[2]

May 29, 1998

[1]Research Associate, Program of Computer Graphics, Cornell University.
[2]Professor, Sibley School of Mechanical and Aerospace Engineering, Cornell University.

Abstract

This report describes the spectroradiometric calibration of a CCD camera system, which consists of a high dynamic range (12 bit), liquid cooled scientific grade CCD camera used in conjunction with a series of narrow band and neutral density filters. The ultimate purpose of the calibration is to convert multiple single channel images obtained from the camera into a quantitative spectral image of a viewed scene. The present work extends earlier work [PCG-96-1] in which spectral transmittance curves for the filters and camera lens system were measured, and linearity tests of the CCD sensor output as a function of incident illumination strength, and camera shutter and lens aperture opening, were carried out. The present study specifically extends the prior report to include the effects of focal distance and the spectral response function of the camera. The report provides a comprehensive radiometric model for the camera and describes a method of spectral recreation from camera measurements. The present report also describes and demonstrates a method for converting camera measurements into quantitative colorimetric information in terms of XYZ-CIE matching functions.

Chapter 1

Introduction

This report describes a study of a particular charge coupled device (CCD) camera, the Photometrics PXL1300L. In brief, the report includes linearity tests on the camera, the determination of the spectral response function of the camera, and a method of spectral recreation from camera measurements. The mathematical procedures used to obtain colorimetric information and spectral recreations or reconstructions of an unknown input source spectrum, using camera measurements of the source taken through a range of color filters, are described and demonstrated. Some of the calibration results used in this report are based on a previous technical report from our laboratory [PCG-96-1].

The organization of this report is as follows. Chapters 2 and 3 describe the functionality and the mathematical modeling of a CCD camera. Chapter 4 describes linearity verification over ranges of F-Stops, object distances and shutter speeds. Chapters 5 and 6 describe the mathematical method necessary for colorimetric and spectral recreation. Chapter 7 demonstrates the use of the methods in extracting colorimetric information.

Chapter 2

CCD Camera

A CCD camera has three components: a CCD imager, amplification circuitry and a lens system. CCD stands for *charge-coupled device*. The CCD imager is a particular type of silicon array imaging device containing an array (linear or two dimensional array) of sensor elements. Light falling on the sensor elements (pixels) creates charge (electron-hole pairs) by the photoelectric effect. This charge is collected at each pixel by the formation of a potential well. The amount of charge collected at each pixel is linearly dependent on the light level, the spectral distribution of the light, and the exposure time, at least until the potential well capacity is exceeded. For output, the collected charge is converted to voltage by an amplifier circuit.

Most CCD imagers have a silicon substrate. Silicon is opaque to light with wavelengths shorter than 400nm and transparent to light beyond 1100nm. So a CCD imager is useful only in the range where some light is absorbed, namely, in the range between 400nm and 1100nm. Within this range, different wavelengths have different capacities for creating charge from incident photons. This capacity is measured in terms of *quantum efficiency* (see Figure 2.1) which indicates what percentage of photons of a particular wavelength hitting the front face of the CCD is converted into an electric charge. The quantum efficiency is always less than one and varies with the wavelength of light and the construction of the imager.

In addition to the action of light, thermal agitation in the silicon substrate also gives rise to charge inside the sensor element. This charge, being indistinguishable from those generated by the effect of light, introduces noise in the CCD output. This noise is called dark signal or *dark current*. Because of its thermal origin this noise, known as *thermal noise*, can be controlled by cooling the CCD device to a lower temperature.

The sensitivity of a CCD is given by the signal-to-noise ratio, which in turn is determined by two parameters: the quantum efficiency of the CCD and its noise. For short integration times the noise of a CCD is usually given by its readout noise, the least amount of noise associated with any pixel. In such a case any two CCDs can be directly compared by taking the ratio of quantum

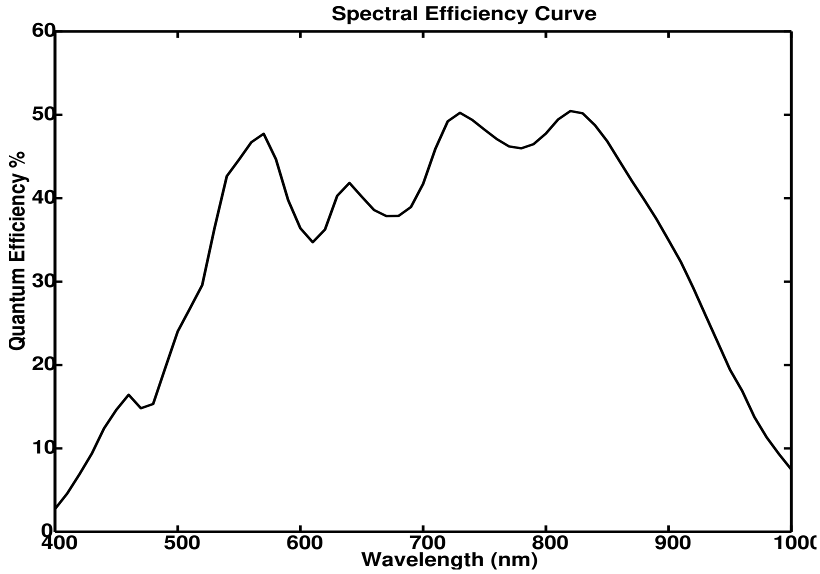

Figure 2.1: Spectral quantum efficiency curve of Kodak KAF-1300L CCD imager (manufacturer supplied).

efficiency to readout noise. For longer integrations dark current noise dominates, so sensitivity as measured by the ratio of quantum efficiency to dark current is relevant.

The particular CCD camera used in the Light Measurement Lab (LML) is a Photometrics PXL 1300. The various units of the camera are:

- Photometrics PXL Camera Head. It utilizes a liquid cooled Kodak KAF1300L[1] scientific grade CCD image sensor containing a 2-D array of sensor elements.
- Photometrics PXL Camera Electronics Unit.
- Photometrics PXL Liquid Cooling Unit.
- Nikon lens (Micro-NIKKOR, Focal Length = 55mm, 1:2.8). The lens transmits in the wavelength range of 350nm - 900nm and beyond 1000nm. The spectral transmittance curve is shown in Figure 2.2.

The various features of the camera system are given in Table 2.1.

[1] "KAF1300L CCD sensor is built with a two-phase, two-polysilicon, NMOS CCD technology. This technology aids in the reliable fabrication of small pixel sizes. It aids in lowering the dark current without compromising charge capacity." Kodak KAF-1300L Manual.

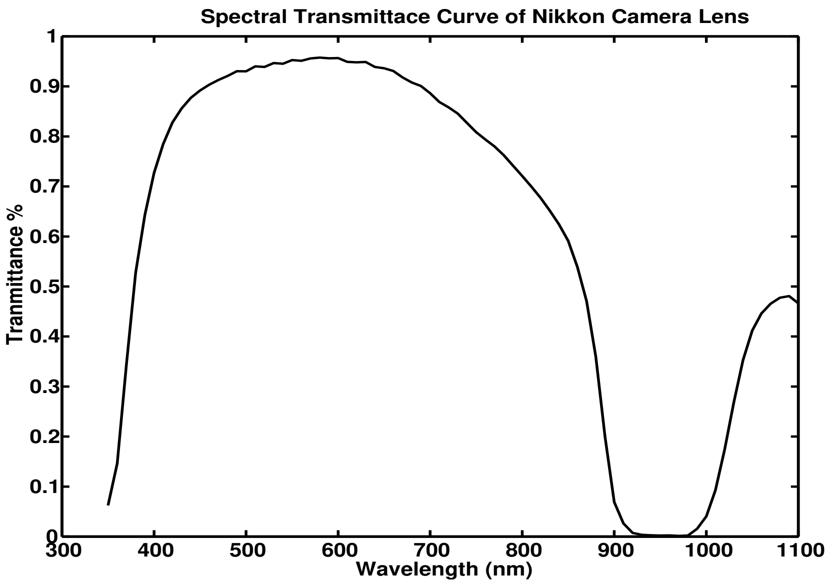

Figure 2.2: Measured spectral transmittance of Micro-NIKKOR (55mm, 1:2.8) lens.

Resolution	1280 (H) $\times$ 1024 (V) pixels.
Pixel size	16 μ $\times$ 16 μ.
Saturation Signal	150,000 electrons.
Quantum Efficiency (shown in Figure 2.1)	11% at 450nm. 40% at 550 nm. 40% at 650 nm.
Useful Spectral Range	400nm-1000nm.
Output Sensitivity	10 μV/electron.
Dark Current	0.05electrons/pixel/sec at -40^{0}C. Dark current doubles every 6^{0}C increase.
Dynamic Range (Saturation Signal/Dark Noise)	75 dB.
Digitization	12 bits pixel value range : 0 to 4095.

Table 2.1: KAF1300L CCD imager characteristic.

Chapter 3

Quantitative Radiometry with CCD Camera

As mentioned earlier, photons are absorbed in the CCD sensor elements and generate electrons by the photoelectric effect. These electrons are then stored in the potential well and, subsequently, are passed through an amplification circuitry which gives rise to a signal. Thus the signal read from any CCD sensor is directly proportional to the accumulated charge in the potential well of the sensor and in turn is proportional to the number of photons incident on the sensor area. So, in principle, we can use each CCD pixel as a radiometer, *i.e.*, we can use the signal to derive quantitative information about the incident light. In this chapter we will derive expressions for extracting this information.

3.1 Noise Correction

Before proceeding to derive quantitative information, we will consider the noises introduced in the signal measurement. These noises must be accounted for before carrying out any data acquisition. We shall categorize the noises into two types: additive and multiplicative.

3.1.1 Additive Noise

The additive noise is an additive signal which merges with the useful signal. The best known additive noise is *thermal noise.* It is possible to reduce thermal noise by deeply cooling the CCD imager. The other additive noise is *preamplifier noise*, which is generated by the on-chip output amplifier. This noise is present even in the absence of thermal noise. A simple and efficient method of suppressing the effect of the additive noise (both components) is to obtain a signal (S_d) in complete darkness, with the same operating temperature and the same exposure time as the original image signal (S_o) to be corrected, and subtract S_d from S_o.

3.1.2 Multiplicative Noise

Multiplicative noise results from variations in sensitivity from one sensor to another. This corresponds to the variation of the sensor characteristics over the imager surface. The cause could be many: *e.g.*, thickness variation of the CCD chip, dust on the imaging optic surface, optical vignetting, *etc.* Correction of this noise requires the measurement of a shading correction frame or *flat field.* A flat field (S_f) corresponds to the measured signals obtained by viewing a uniform light field, *e.g.*, by imaging an integrating sphere uniform light source. Using the flat field signal, the corrected signal is obtained as:

$$S = \frac{S_o - S_d}{S_f - S_d} S_{fa}$$

where

S is the noise corrected signal for a given pixel,

S_o is the measured source image signal,

S_d is the additive noise (thermal + preamplifier),

S_f is the flat field signal,

S_{fa} is the average signal of the flat field.

After the correction is made then the generated signal is independent of the pixel position and every pixel on the CCD imager may be considered to be an independent radiometer.

3.2 Acquiring Image using the PXL Camera

As said earlier, the PXL imaging system has a camera optical unit attached to it, which helps in acquiring an image. Imaging is done by electronically opening and closing the camera shutter. Camera shutters are mechanical and hence their opening and closing take times on the order of milliseconds. The camera shutter in the PXL is mechanical (5 leaf iris). So during opening of the shutter, the CCD imaging chip area is gradually exposed to the incoming photons and, similarly, during the closing of the shutter, the chip area is gradually covered from the exposure to the photons. It would be nice if the electronics could be set so as to start acquiring the photoelectric charge only after the shutter is fully open and then stop acquiring the charge when the shutter starts to close. However, our CCD camera (PXL) does not provide this convenience. When the camera is instructed to acquire, the electronics become active to acquire the charges independent of whether the shutter is fully open or closed. Because of the gradual opening and closing of the shutter, the effective acquiring time becomes a little *less* than the specified acquiring time. To help offset this problem the CCD system allows the camera user to specify an open delay time and a close

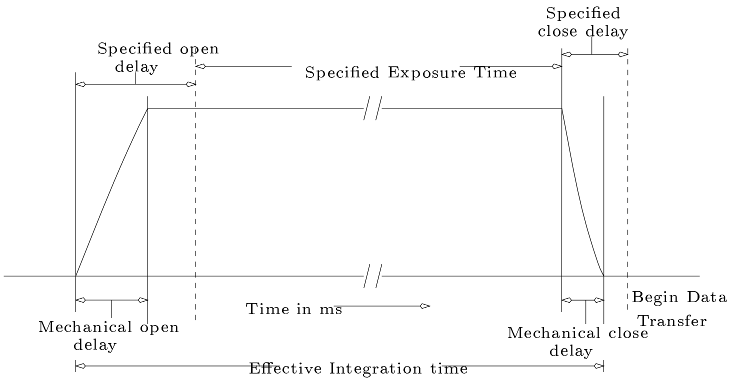

Figure 3.1: Image aquiring using PXL CCD camera.

delay time (see Figure 3.1). The recommended open and close delay times for the present camera are 15 and 30 msecs respectively. The CCD starts acquiring as usual, but the clock which counts the time of exposure becomes active only after the specified open shutter delay time. After the specified time of exposure is passed the mechanical shutter is signaled to close. But the system waits for the specified close shutter delay time before the acquired image data is transferred. This procedure assures that photons are acquired at least up to the specified exposure time (but could be longer).

One way to guarantee that all the pixels uniformly acquire photons during a given period of time t, is to take measurements at two different exposures: one at time t_1 and the other at time $t_1 + t$ and subtract the former from the latter. The method has a small disadvantage because we lose the full 12 bit capacity of the CCD imager. Another way is to determine the excess exposure time, Δt, for each pixel in a calibration stage and to make a pixelwise correction for this known excess in every measurement. The first procedure is used in the present report.

3.3 Imaging Model

We have mentioned in the beginning of this chapter that the pixel signal is proportional to the number of photons incident on the sensor area, *i.e.*,

$$S \propto N_{photon}$$

However, the proportionality expression is not this straightforward. Photons of different wavelengths have different capacities to generate photoelectrons. This difference gives rise to a *quantum efficiency* spectrum. So, the same number of photons at two different wavelengths are very likely to generate two different signals. As light is normally a mixture of different wavelengths, the proportionality expression can be written as:

$$S \propto \int_{\lambda_a}^{\lambda_b} Q(\lambda) \cdot N_p(\lambda) \cdot d\lambda$$

where

$Q(\lambda)$ is the quantal efficiency at wavelength λ, and

$N_p(\lambda)$ is the number of photons of wavelength λ incident on the pixel.

The number of photons incident on a pixel at any wavelength depends on many factors, such as the strength of the source light, the characteristics of the camera optics, the time of exposure, *etc.* In the following paragraphs we will discuss these various factors and then proceed to derive an expression for the number of photons incident on a pixel element.

3.4 Camera Lens System

The particular lens system used in our CCD camera is a Micro-NIKKOR (Nikon) with a focal length of 55mm (1:2.8). It is constructed from a series (two) of individual glass lenses and an aperture stop centered on a common axis. This aperture stop is an opaque element with a roughly circular opening to permit the passage of light. The size of the aperture stop is set by the operator of the CCD camera and serves to provide control over the quantity of light striking the CCD imager plane.

Focusing the camera is done by moving the whole lens system along the axis. The amount by which the lens system is moved away from the image plane depends on the distance of the object to which the camera is focused. The closest distance is one when the camera is focused at ∞.

Object Distance (D) (in ft)	15	7	5	4	3	2.5	2	1.75	1.5	1.25	1
Lens shift (**d**) from image plane(in mm)	1	2	3	3.5	5	5.5	7	9	11	14	20

3.5 Radiometry

Assuming that the source image has a constant emission over an exposure period, the number of photons at a wavelength λ falling on a pixel area is proportional to the exposure time and to the pixel irradiance at wavelength λ.

$$N_p(\lambda) = t \cdot \mathcal{F}(\lambda) \cdot \int_{\text{Pixel\_Area}} E(\lambda) dA' \tag{3.1}$$

where

t is the exposure time (in seconds),

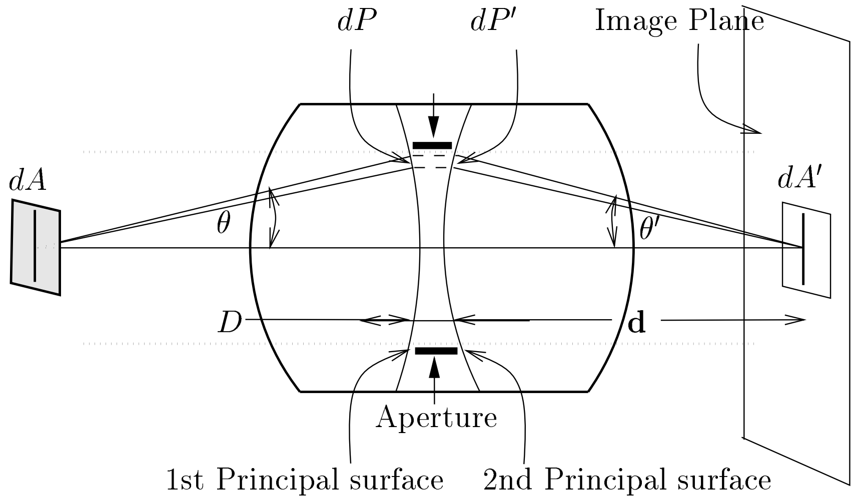

Figure 3.2: Camera imaging of a differential source dA at dA' of camera imager plane.

$\mathcal{F}(\lambda)$ is a factor for converting light energy expressed in Joules to number of photons and is equal to $1/h\nu$, where h is Plank's constant and ν is the frequency of light,

$E(\lambda)$ is the irradiance at differential area dA' of the pixel.

Let the radiance of the source A be $L(\lambda)$ (watt ster^{-1} m^{-2}). The projected area of the source in the direction θ is $dA\cos\theta$ (m^{-2}). The solid angle subtended by the differential area dP from dA is dP/D^2, where D is the distance from the object to the first principal surface. Therefore the radiant power intercepted by the area dP is

$$\text{Power} = L\frac{dP}{D^2}dA\cos\theta \quad \text{(watt)}$$

This power is transmitted to the differential area dP' on the 2nd principal surface and is then imaged by the optical system to area dA', with a projected area $dA'\cos\theta'$, and with a solid angle $dP'/\mathbf{d}^2$. Thus the radiance seen at dA' is

$$L'(\lambda) = T(\lambda)L(\lambda)\frac{dP}{D^2}dA\cos\theta\left[\frac{\mathbf{d}^2}{dP'\,dA'\cos\theta'}\right] \quad \text{(watt ster}^{-1}\text{ m}^{-2}\text{)}$$

where $T(\lambda)$ is the spectral transmission of the optical system.

The differential areas dA and dA' are related by 1st order optics as

$$dA\cdot\mathbf{d}^2 = dA'\cdot D^2.$$

Further

$$dP\cos\theta = dP'\cos\theta'.$$

Substituting these, the above radiance equation simplifies:

$$L'(\lambda) = T(\lambda)L(\lambda).$$

Then the expression of the differential irradiance at $\mathrm{d}A'$ due to radiance at dP' will be

$$dE(\lambda) = L'(\lambda)\frac{dP'}{\mathbf{d}^2}\cos\theta'.$$

Integration over the whole area of the optical (source image) surface visible through the aperture stop will give the total irradiance at $\mathrm{d}A'$. The location of the plane of the aperture stop is sketched in Figure 3.2. So the expression of the total irradiance will be:

$$E(\lambda) = T(\lambda)L(\lambda)\frac{\text{Aperture\_area}}{\mathbf{d}^2} \quad (\text{watt m}^{-2})$$

The foregoing expression is only valid for an ideal optical imaging condition and for a differential area around a point where the principal axis meets the image plane. For areas away from that point the irradiance expression becomes very complicated. If we assume a small aperture stop then irradiance can be shown to decrease simply by a $\cos^4\alpha$ factor where α is equal to the angle between dA' and the center of the aperture. The general expression for the irradiance becomes:

$$E(\lambda) = T(\lambda)L(\lambda)\frac{\text{Aperture\_area}}{\mathbf{d}^2}\cos^4\alpha$$

The aperture area is known to be inversely proportional to the square of the F-stop number, F.

Now assuming the irradiance to be uniform over the pixel area we can rewrite the expression for the photon count as:

$$N_p(\lambda) \propto t \cdot \mathcal{F}(\lambda) \cdot T(\lambda) \cdot L(\lambda) \cdot F^{-2} \cdot \mathbf{d}^{-2} \cdot \cos^4\alpha \cdot \text{Pixel\_area} \qquad (3.2)$$

After wavelength integration, the expression for the signal generated at a pixel is:

$$S = C \cdot t \cdot F^{-2} \cdot \mathbf{d}^{-2} \cdot \cos^4\alpha \cdot \int_{\lambda_a}^{\lambda_b} \mathcal{F}(\lambda) \cdot Q(\lambda) \cdot T(\lambda) \cdot L(\lambda) \cdot d\lambda,$$

where C is called the camera constant, which subsumes the Pixel_area, the proportionality between the Aperture_area and the inverse square of the F-stop, and the amplification factor of the CCD amplifier circuit.

The $\cos^4\alpha$ factor in the above equation gives the variation of the pixel value as a function of its position in the image plane. This variation is actually compensated during the flat field correction. Hence, for measurements with a flat field correction we can write the final expression for the pixel signal as:

$$S = C \cdot t \cdot F^{-2} \cdot \mathbf{d}^{-2} \cdot \int_{\lambda_a}^{\lambda_b} \mathcal{F}(\lambda) \cdot Q(\lambda) \cdot T(\lambda) \cdot L(\lambda) \cdot d\lambda. \qquad (3.3)$$

Chapter 4

CCD Camera Calibration

In Equation (3.3) we have set up a simple, but fairly complete, mathematical model relating the pixel signal to various factors. The validity of this model must be verified before carrying out any quantitative measurements. In other words we have to calibrate the CCD camera against each variable parameter, keeping all other parameters fixed. We provide here a summary of the calibration results of our PXL Photometrics camera.

4.1 Calibration for Exposure Time Dependence

Pixel signal and exposure time are linearly related in our model. Hence the plot of signal *vs* time should be a straight line. Figure 4.1 shows two such results measured at two different source-photon strengths with manufacturer recommended shutter delays. The exposure time was corrected for individual pixel exposure variations by taking the difference between two measurements. The plots are almost exactly linear with a zero intercept, and hence agree with the model.

4.2 Calibration for F-Stop Dependence

In our signal equation (Equation 3.3) we have an inverse square relationship between the measured signal and the F-Stop of the camera, *i.e.*, $S \propto F^{-2}$. A plot of signal versus F^{-2} in Figure 4.2 verifies this relationship. The only significant departure from linearity is for the largest lens opening shown, corresponding to an F-stop value of 5.6 (the rightmost data point in the figure), where other lens corrections may become important.

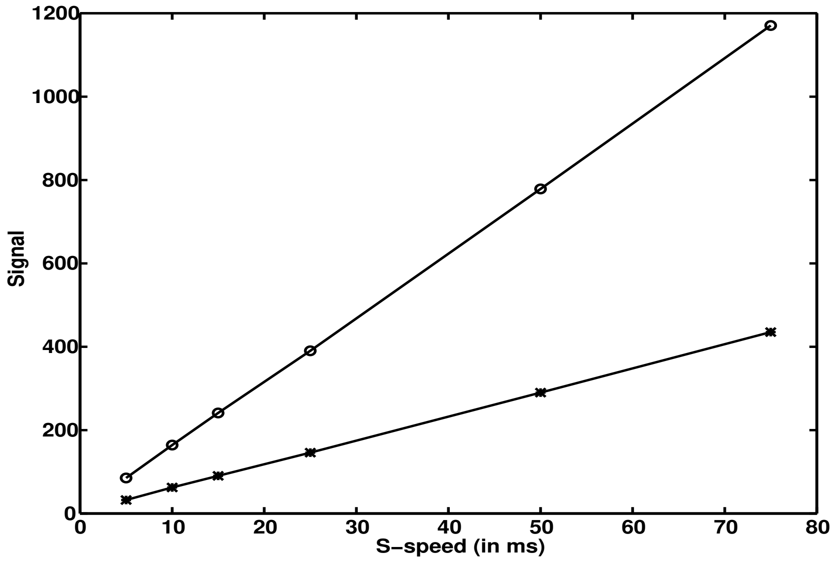

Figure 4.1: Signal linearity as a function of exposure time.

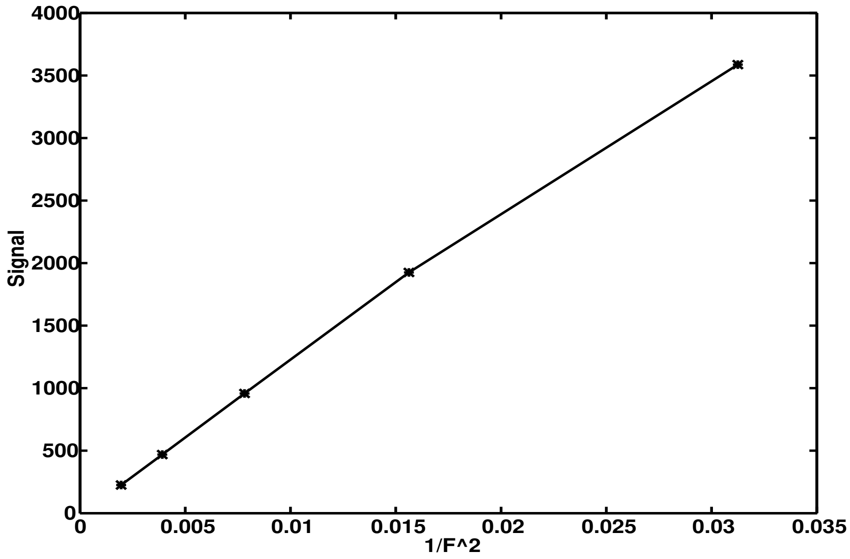

Figure 4.2: Signal as a function of F-stops.

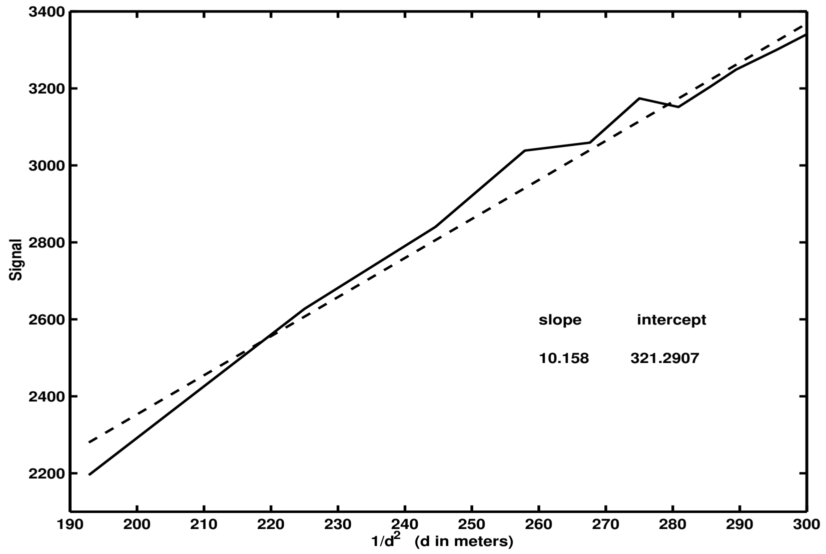

Figure 4.3: Signal as a function of focal distance **d**.

4.3 Calibration for Source Distance

Similar to the effect of F-stop, the signal has an inverse square relationship with the focal distance **d**, of the camera. A plot of signal versus $\mathbf{d}^{-2}$ in Figure 4.3 establishes this relationship.

4.4 Calibration for Source Radiance Dependence

Source radiance $L(\lambda)$ is a function of wavelength. Most sources emit light over a range of wavelengths. For such sources, keeping the wavelength distribution fixed, if we vary the amplitude then our model predicts a linear relationship. This relationship can be established by using neutral density filters in front of the camera lens. Several neutral density filters were available, each with essentially a uniform transmittance across the wavelength range of the camera. Figure 4.4 shows a plot of signal *vs* photon density. Exactly similar measurements have been carried out using monochromatic light sources at a few wavelengths and the same linearity has been observed.

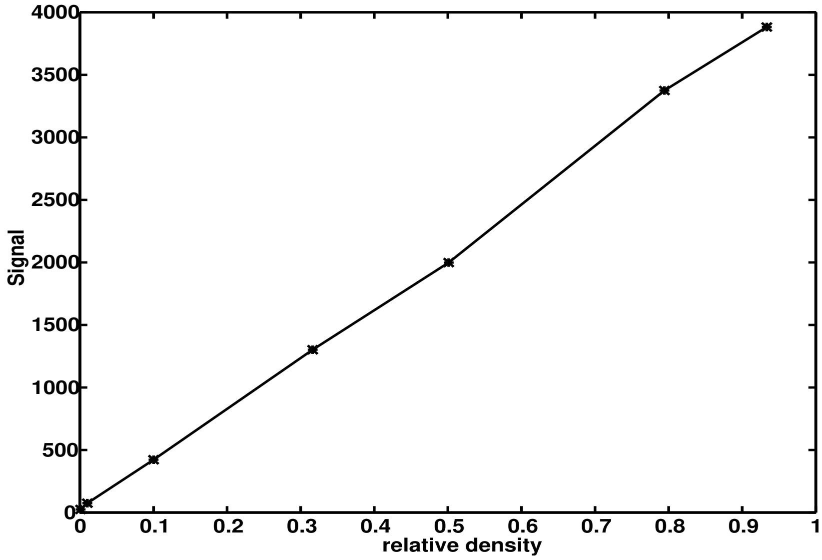

Figure 4.4: Linearity of signal strength as a function of photon density.

Chapter 5

Extraction of Colorimetric Information

The CCD signal modeled by Equation (3.3) does not provide any colorimetric information. In this chapter we describe a method for computing colorimetric information in XYZ coordinates from the CCD pixel signals.

The colorimetric quantities X, Y, and Z for a light source (target) of spectral distribution $L(\lambda)$ are given by :

$$X = \int_{\lambda_1}^{\lambda_2} L(\lambda)\bar{x}(\lambda)d\lambda;\ Y = \int_{\lambda_1}^{\lambda_2} L(\lambda)\bar{y}(\lambda)d\lambda;\ Z = \int_{\lambda_1}^{\lambda_2} L(\lambda)\bar{z}(\lambda)d\lambda \tag{5.1}$$

where $\bar{x}(\lambda)$, $\bar{y}(\lambda)$ and $\bar{z}(\lambda)$ are the CIE ideal observer color matching functions. The equations imply that we have to know the target spectrum to compute the colorimetric quantities. We show below that it is possible to derive the colorimetric values of an unknown target by taking multiple measurements through narrow band filters.

A simplified expression for the CCD pixel signal given by Equation (3.3) after measurement through a narrow band filter can be written as:

$$S_i = K \int_{\lambda_1}^{\lambda_2} L(\lambda)F_i(\lambda)d\lambda \tag{5.2}$$

where

S_i is the time factored signal (*i.e.*, signal strength at unit time),

$K = C \cdot F^{-2} \cdot d^{-2}$,

$F_i(\lambda) = \mathcal{F}(\lambda) \cdot Q(\lambda) \cdot T_i(\lambda)$, and

$T_i(\lambda)$ is the spectral transmittance of the camera lens and i-th narrow band filter.

$F_i(\lambda)$ can be obtained from the manufacturer supplied CCD chip response function and the lens and filter transmittance data measured independently. K, the proportionality constant, is dependent on the measurement time, camera focus setting and aperture setting, and so can be computed from measurements using a calibrated light source.

Given sufficient narrow band filter and lens combinations we can express the color matching functions $\bar{x}(\lambda)$, $\bar{y}(\lambda)$ and $\bar{z}(\lambda)$ as linear combinations of the $F_i(\lambda)$'s. *i.e.*,

$$\bar{x}(\lambda) \approx \sum_i b_i^x F_i(\lambda); \quad \bar{y}(\lambda) \approx \sum_i b_i^y F_i(\lambda); \quad \bar{z}(\lambda) \approx \sum_i b_i^z F_i(\lambda). \tag{5.3}$$

Substituting these in Equation (5.1) we will get the expressions for X, Y and Z in terms of the CCD pixel signals. The resulting expression for X is given below.

$$\begin{aligned} X &\approx \int_{\lambda_1}^{\lambda_2} L(\lambda) \sum_i b_i^x F_i(\lambda) d\lambda \\ &= \sum_i b_i^x \int_{\lambda_1}^{\lambda_2} L(\lambda) F_i(\lambda) d\lambda = \frac{1}{K} \sum_i b_i^x S_i. \end{aligned}$$

Similarly,

$$Y \approx \frac{1}{K} \sum_i b_i^y S_i \qquad \text{and} \qquad Z \approx \frac{1}{K} \sum_i b_i^z S_i. \tag{5.4}$$

Thus from a linear combination of the CCD measurements taken through a set of narrow band filters we can compute the colorimetric values of a target. The accuracy of this computation will depend on how well the CIE matching functions are approximated by the narrow-band filter functions.

Chapter 6

Spectral Extraction

In Equation (3.3) we have derived the relationship between the source radiance and the measured signal. Radiance is a function of wavelength. Though it is impossible to invert Equation (3.3) to compute the spectral radiance, it may be possible to compute an approximation to the spectrum from a series of measurements. Here we provide a method to compute this approximation. It is based on a projection method.

Projection is a standard tool for handling functions. Using this tool, one reduces the dimensionality of the function from infinite to finite. In the process one generates an approximation of the original function. The source-target radiance, $L(\lambda)$, is approximated by the following expression:

$$L(\lambda) \approx \sum_{j}^{n} L_j B_j(\lambda) \tag{6.1}$$

where B_j's are a finite set of n known functions called *basis functions*. The multipliers, L_j's, in the above equations are called coefficients of approximation. As the basis functions are known functions, the finite set $\{L_j\}$ is taken as the new representation of the function and the size of this set is the dimension of this new representation. With a proper choice of number and types of basis functions it is possible to get a fair approximation to any given class of functions.

If we replace $L(\lambda)$ in Equation (5.2) by the expression given in Equation (6.1) we will get

$$S_i = K \sum_{j}^{n} L_j \int_{\lambda_a}^{\lambda_b} F_i(\lambda) B_j(\lambda) d\lambda = K \sum_{j=1}^{n} L_j b_{ij}, \tag{6.2}$$

where $b_{ij} = \int_{\lambda_a}^{\lambda_b} F_i(\lambda) B_j(\lambda) d\lambda$.

We can now proceed to set up a system of m linearly independent equations with n unknown L_j's by measuring signals with m different lens-and-filter transmittance functions $T_i(\lambda)$. The variation of the lens-and-filter transmittance function can be carried out by using m color filters during the measurements. The system of linear equation is shown below:

$$\begin{bmatrix} S_1 \\ \vdots \\ S_m \end{bmatrix} = K \cdot \begin{bmatrix} b_{11} & ... & b_{1n} \\ \vdots & \vdots & \vdots \\ b_{m1} & ... & b_{mn} \end{bmatrix} \cdot \begin{bmatrix} L_1 \\ \vdots \\ L_n \end{bmatrix} \tag{6.3}$$

Solution of the linear equations will give us the coefficients $\{L_j\}$ as:

$$\begin{bmatrix} L_1 \\ \vdots \\ L_n \end{bmatrix} = \frac{1}{K} \cdot \begin{bmatrix} b_{11} & ... & b_{1n} \\ \vdots & \vdots & \vdots \\ b_{m1} & ... & b_{mn} \end{bmatrix}^{-1} \cdot \begin{bmatrix} S_1 \\ \vdots \\ S_m \end{bmatrix} \tag{6.4}$$

Substituting these in Equation (6.1) will yield an approximation to the unknown source-target radiance $L(\lambda)$.

When $m = n$ and the filter functions $T_i(\lambda)$ are linearly independent, the inversion is straightforward. Otherwise one has to carry out the inversion using a pseudo-inversion method based on singular value decomposition. (MATLAB provides a PINV function to carry out such pseudo-inverse computation.)

6.1 Choice of Basis Functions

One can imagine a large number of possible basis functions, but there is no clear cut choice about what would be the best basis set. An arbitrary basis set might not give a good approximation to the unknown source-target radiance function. Further, there may not be a best basis set for arbitrary source-target radiance functions. Under this situation it seems that a reasonable basis set might be the one which represents the functions $F_i(\lambda)$ exactly. As $F_i(\lambda)$'s are known functions, involving the lens and filter transmittances $T_i(\lambda)$ and the CCD energy efficiency factor $\mathcal{F}(\lambda)Q(\lambda)$, it is possible to derive such a basis set by an orthogonalization method.

Chapter 7

Measurements and Computation

We describe below some of the measurements and computations that we carried out to compute colorimetric images of a physical scene. The reconstructed images were used to compare with a synthetic image of the same scene.

Figure 7.1 shows the measurement setup. The box on the left of the figure is

Figure 7.1: Measurement setup.

the physical environment illuminated with a controlled light source. The setup on the right is the CCD camera system of interest. Measurements were carried out by placing the narrow-band filters in front of the camera. The transmittance spectra of the filters is shown in Figure 7.2. The filters have approximate half

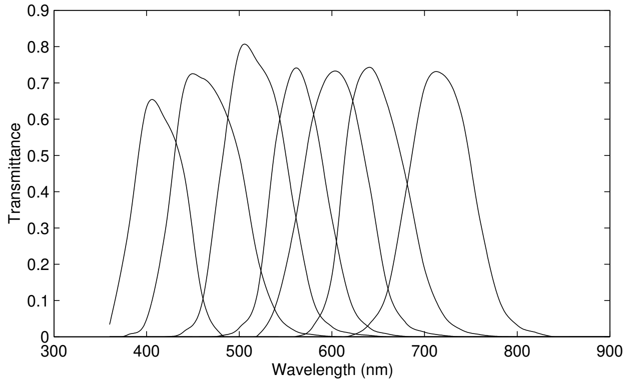

Figure 7.2: Transmittance spectra of the 7 narrow-band filters.

band-widths of 50nm and have peak transmittances at 400, 450, 500, 550, 600, 650 and 700 nm, respectively. The approximation of the CIE matching functions computed from Equation (5.3) using these 7 narrow-band filters along with the camera lens transmittance (Figure 2.2) and the CCD light energy efficiency function (Figure 2.1 times the conversion factor $\mathcal{F}(\lambda)$) is shown in Figure 7.3.

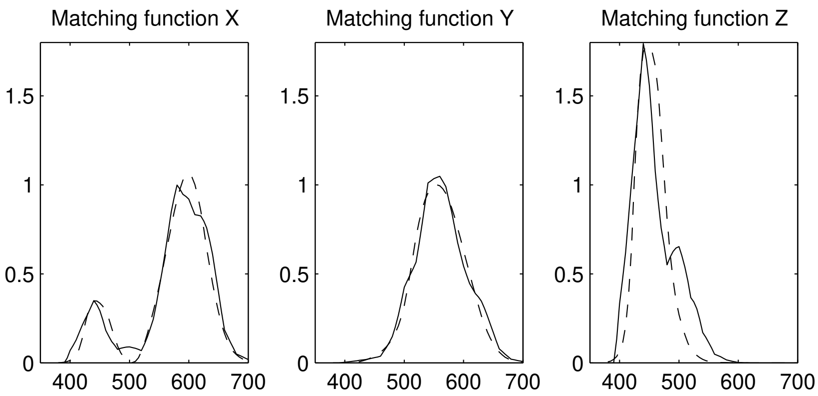

Figure 7.3: Approximate CIE matching functions (solid lines) and actual matching functions (dotted lines).

The flat field calibration was done by viewing the exit port of a uniform light source with the CCD camera. The reference light source is a 12" diameter calibrated integrating sphere (shown in Figure 7.4) which is designed to provide uniform light over its full 4" diameter circular exit port. The uniformity is greater than 98%. The exact procedure used for the flat field calibration will

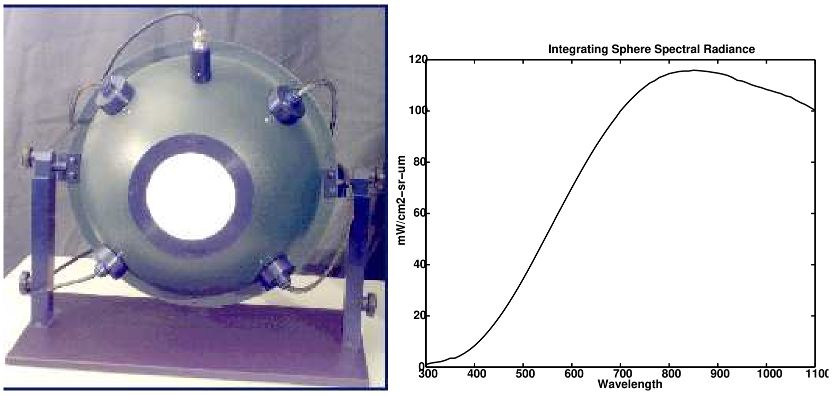

Figure 7.4: Integrating sphere light source and its calibrated spectrum.

be discussed in another report [Steve]. The spectral power output of the light source is shown on the right in Figure 7.4. This calibrated spectrum is used to compute the camera constant for quantitative work.

Seven measurements of the Cornell Box scene were done with the CCD camera and filter combinations. To compensate for the spectral variation of the CCD chip sensitivity and the light source spectral power output, different exposure times were required to get CCD image signals at near 12 bit capacity. (The exposure times for the filters with peaks at 400, 450, 500, 550, 600, 650, and 700 nm were 100, 0.75, 0.2, 0.1, 0.075, 0.05 and 0.075 seconds, respectively[1].) Tristimulus values were computed by applying Equations (5.3) and (5.4) to the pixel-signals of the seven measured images.

Figures 7.5, 7.6 and 7.7 list the MATLAB programs used for computing, respectively, the multiplication factors for a linear combination of 7 measurements, the camera constant at a particular camera setting, and the tri-stimulus images of the Cornell box. The multiplication factors, b_i^x's, b_i^y's, and b_i^z's for Equation (5.4), computed using the program are: [16.669 1.9148 0 1.1524 6.9177 0 0], [1.0469 0 5.8237 3.0806 2.7977 0 0] and [78.7146 14.3586 0 0 0 0 0]. The constant K in Equation (5.2) is computed from a set of measurements at F-Stop=16 as 457.68. The image on the left of Figure 7.8 shows an RGB color image computed by color-space transformation of the tristimulus values obtained using the program listed in Figure 7.7.

[1] Recall that the additive (thermal or dark current) noise in the imager increases with exposure time, so that this noise is greatest for the filter measurements at short wavelengths.

```
function [cX,cY,cZ] = combination_factors()
%
% Compute linear combination factor for 7 filter CCD measurements
% to generate CIE tri-stimulus values (X,Y,Z) of the measured light source.
[X,Y,Z,lambda_XYZ] = get_XYZ; % get Tri-strimulus response function data.
%
% Quantal Efficiecy of the CCD chip. As provided by the Manufacturer.
Quant_eff = [0         0    2.7262    4.5846    6.9099    9.3752   12.3971 ...
   14.6141   16.4340   14.8158   15.3257   19.6840   24.0263   26.7845 ...
   29.5855   36.3664   42.6439   44.6308   46.7100   47.7365   44.6948 ...
   39.7790   36.3939   34.7148   36.2459   40.2827   41.8437   40.1703 ...
   38.5798   37.8546   37.8727   38.9440   41.7185   45.9209   49.2163 ...
   50.2404   49.3917   48.2287   47.0943   46.2036   45.9869   46.4835 ...
   47.7591   49.4473   50.4596   50.1918   48.7579   46.8426   44.4647 ...
   42.0801   39.8541   37.5268   34.9810   32.3554   29.2819   26.0035 ...
   22.7539   19.4374   16.8918   13.7415   11.3124    9.3019    7.4702]/100;
lambda_quantal = [380:10:1000];
%  Number of quanta per joule of energy at wavelength lambda (in m) :
% 1/(h*nu) = lambda/(h*C)
% where h : planc's constant=6.6262*10^(-34)J.S, C : speed of light=299792458m/s
quanta = (lambda_quantal*1e-9)/(6.6262*1e-34*299792458); coulombs = quanta/6.24e18;
Power_eff = Quant_eff .* coulombs;
%
%  Lens transmittance Measured from 350nm to 1100nm at 10nm interval.
% Lens measured : 55mm NIKON
%  It is assumed that most of the NIKON lenses have similar transmittance.
lens_trans=[0.0634    0.1521    0.3584    0.5363    0.6649    0.7488 0.8053 ...
    0.8459    0.8722    0.8919    0.9048    0.9175    0.9247    0.9331 ...
    0.9404    0.9409    0.9498    0.9493    0.9563    0.9553    0.9624 ...
    0.9611    0.9655    0.9673    0.9653    0.9622    0.9578    0.9579 ...
    0.9590    0.9496    0.9471    0.9426    0.9309    0.9207    0.9141 ...
    0.9001    0.8841    0.8732    0.8611    0.8435    0.8255    0.8115 ...
    0.7981    0.7805    0.7602    0.7405    0.7195    0.6965    0.6713 ...
    0.6431    0.6105    0.5564    0.4857    0.3711    0.2061    0.0712 ...
    0.0272    0.0077    0.0038    0.0027    0.0023    0.0024    0.0014 ...
    0.0023    0.0159    0.0419    0.0961    0.1808    0.2805    0.3705 ...
    0.4342    0.4722    0.4940    0.5073    0.5122    0.4977];
lambda_lens= [350:10:1100];
filter_trans = [0.0340 0.2880 0.6330 0.6000 0.4560 0.1140 0.0080 zeros(1,31);
0 0.0060 0.0480 0.2890 0.6810 0.7130 0.6490 0.4990 0.2170 0.0670 0.0170 0.0060 ...
0.0010 zeros(1,25); zeros(1,4) 0.0140 0.0950 0.4570 0.7870 0.7570 0.6460 0.3460...
0.0990 0.0280 0.0100 0.0040 zeros(1,23); zeros(1,6) 0.0030 0.0250 0.1250 0.5450 ...
0.7400 0.6160 0.3260 0.0980 0.0260 0.0080 0.0010 zeros(1,21); zeros(1,8) 0.0040 ...
0.0910 0.3120 0.6100 0.7300 0.6710 0.4260 0.1370 0.0380 0.0130 0.0040 zeros(1,19);
zeros(1,11) 0.0300 0.1680 0.6170 0.7430 0.6390 0.4370 0.1880 0.0620 0.0190 ...
0.0060 0.0010 zeros(1,16); zeros(1,13) 0.0030 0.0340 0.1270 0.4020 0.6870 ...
0.7230 0.6110 0.3200 0.1050 0.0320 0.0120 zeros(1,14)];
lambda_filter=360:20:1100; lambda = [380:5:720]; % Working wavelength
mf=interp1(lambda_lens,lens_trans,lambda).*interp1(lambda_quantal,Power_eff,lambda);
tF = [];
for i = 1:7 tF = [tF;interp1(lambda_filter,filter_trans(i,:),lambda).*mf]; end;
cX =  nnls(tF',interp1(lambda_XYZ',X',lambda'));
cY =  nnls(tF',interp1(lambda_XYZ',Y',lambda'));
cZ =  nnls(tF',interp1(lambda_XYZ',Z',lambda'));
return;
```

Figure 7.5: MATLAB listing for computing the linear combination factors for converting 7 narrow-band measurements to CIE-Tristimulus values. (See Equation 5.4)

.

```
function constant = camera_constant()
%
% Computation of Camera Constant from 7 narrowband filter Measurements
% of Integrating Sphere Light source
% for the Camera setting :
% F16, Focus at 5'. 52mm Nikon Lens.
%
% Measurements were done through 2.0 OD ND filter.
%
% Integrating sphere with only 1 light on
% and filtered through an IR cutoff filter.
%
% Luminance of the light source measured using Minolta photometer:
% direct source : 10100 cd/m^2  approx (it had a 4 digit overflow)
% source viewed through the 2.00D ND filter: 109.4 cd/m^2
%
% Only a small 20x20 area from the center of the image is captured.
% (NOTE : As with any measurement with this CCD camera the left most column
%   is useless and hence to be discarded.)
%

files = {'400.60.0sec';'450.4.0sec';'500.1.2sec';'550.0.75sec';'600.0.5sec';
         '650.0.45sec';'700.0.3sec'};
dark_files = { 'Dark.60.0sec'; 'Dark.4.0sec'; 'Dark.1.2sec'; 'Dark.0.75sec';
                'Dark.0.5sec'; 'Dark.0.45sec'; 'Dark.0.3sec'};
time_in_sec = [60,4,1.2,0.75,0.5,0.45,0.3];
for i = 1:7
  A = iplab_read(files{i});
  D = iplab_read(dark_files{i});
  [rows,cols] = size(A);
  % Data in First column is a always 45 and must be discarded
  signal = (A(:,2:cols)-D(:,2:cols))/time_in_sec(i);
  value(i) = max(signal(:));
end;
%disp(value);
[cfactorX,cfactorY,cfactorZ]=combination_factors;
computed_lum = value*cfactorY;
actual_lum = 109.4; % From photometer measurement.
constant = computed_lum/actual_lum;

return;
```

Figure 7.6: MATLAB listing for computing the constant K for Equation (5.2).

```
function [X,Y,Z]=comp(S)
%
% function [X,Y,Z]=comp(S)
% Computes tri-stimulus values from a set of measurements.

load flat_factor; % Flat field correction factor using Steve Marchsner's method
    % Assumed to be Pre-Computed from separate
    % measurements.

f1 = (iplab_read('cbox.400nm.10sec.f8')-iplab_read('dark.10sec')) ...
        .*flat_factor/10;
f2 = (iplab_read('cbox.450nm.0.75sec.f8')-iplab_read('dark.0.75sec')) ...
        .*flat_factor/0.75;
f3 = (iplab_read('cbox.500nm.0.2sec.f8')-iplab_read('dark.0.2sec')) ...
        .*flat_factor/0.2;
f4 = (iplab_read('cbox.550nm.0.1sec.f8')-iplab_read('dark.0.1sec')) ...
        .*flat_factor/0.1;
f5 = (iplab_read('cbox.600nm.0.075sec.f8'-iplab_read('dark.0.075sec')) ...
        .*flat_factor/0.075;
f6 = (iplab_read('cbox.650nm.0.05sec.f8')-iplab_read('dark.0.05sec')) ...
        .*flat_factor/0.05;
f7 = (iplab_read('cbox.700nm.0.075sec.f8'-iplab_read('dark.0.075sec')) ...
        .*flat_factor/0.075;

[aX,aY,aZ]=combination_factors;
K = camera_constant;
X = (aX(1)*f1+aX(2)*f2+aX(3)*f3+aX(4)*f4+aX(5)*f5+aX(6)*f6+aX(7)*f7)/K;
Y = (aY(1)*f1+aY(2)*f2+aY(3)*f3+aY(4)*f4+aY(5)*f5+aY(6)*f6+aY(7)*f7)/K;
Z = (aZ(1)*f1+aZ(2)*f2+aZ(3)*f3+aZ(4)*f4+aZ(5)*f5+aZ(6)*f6+aZ(7)*f7)/K;

return;
```

Figure 7.7: MATLAB listing for computing X,Y,Z values from a set of Measurements. A resulting RGB image after a color-space transformation is shown in Figure 7.8.

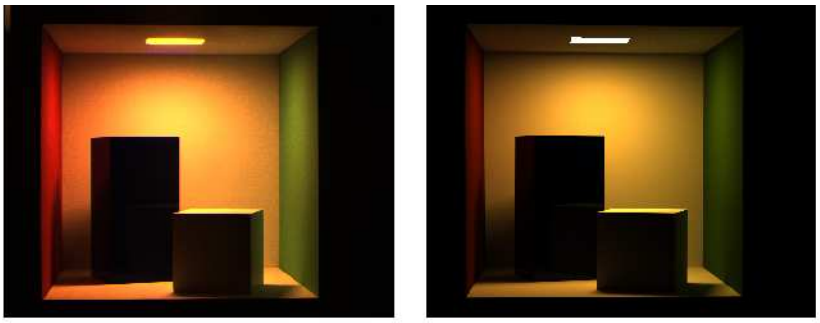

Figure 7.8: Scene images. The image on the left is a measured image and the one on the right is a synthetic image.

7.1 Validation of Rendering Methods

One of the aims of the LML is to develop tools to validate the accuracy of various rendering methods. One way to achieve this would be to measure the illumination of an environment using the CCD camera and to compare the obtained image with a synthetic image of the same environment. The image on the right of Figure 7.8 shows a synthetic image computed using The Particle Tracing Method [Walter97] using an accurate numerical definition of the same scene. The CCD camera pose for Figure 7.8 was extracted by using a pose computation technique developed by Tsai [Tsai86]. This technique has been used successfully in the LML for synthetic camera view specification as required by the rendering method.

Chapter 8

Future Work

The spectral reconstruction technique needs further verification. We have recently come across the work of researchers [Vora97] using 31 narrow band measurements for spectral reconstruction using a similar CCD camera and 31 interference filters. Though we have not come across any report of difficulty in reconstructing from a smaller number of filters, good reconstruction from seven filter measurements may be too optimistic. At the same time reconstruction using a large number of measurements is very laborious and could be error-prone for many reasons (including the possible physical displacement of the camera during filter changes). So further experiments are necessary to find out the minimum number of filters necessary for a good spectral reconstruction.

Chapter 9

Acknowledgements

We acknowledge the generous help of Bruce Walter for generating the synthetic image and of Steve Marschner for providing us a tool to carry out the camera pose calibration and for his help during the measurements. This work was supported by the NSF Science and Technology Center for Computer Graphics and Scientific Visualization (ASC-8920219) and by NSF Metacenter Regional Alliance (ASC-9523483), and performed on workstations generously donated by the Hewlett-Packard Corporation.

Bibliography

[PCG-96-1] Steve S-F. Chen, Jerry Wei-Chieh Li, Kenneth E. Torrance, Sumanta N. Pattanaik, *Preliminary Calibration of the Photometrics PXL1300L CCD Camera*, Technical report, no. PCG-96-1, Program of Computer Graphics, Cornell University, 1996.

[Tsai86] Roger Y. Tsai, *An efficient and accurate camera calibration technique for 3D machine vision.*, Proceedings of IEEE Conference on Computer Vision and Pattern Recognition, 1986, pp. 364-374.

[Steve] Steve Marschner and Steve Westin. Personal communication.

[Vora97] Vora, P. L., Harville, M. L., Farrell, J. E., Tietz, J. D., and Brainard, D. H. (1997). Image capture: synthesis of sensor responses from multispectral images. Proceedings of the 1997 IS&T/SPIE Conference on Electronic Imaging, (San Jose, CA, February 10-14, 1997), 3018, 2-11.

[Walter97] Bruce J. Walter, Philip M. Hubbard, Peter Shirley, and Donald P. Greenberg. *Global illumination using local linear density estimation*, ACM Transactions on Graphics, 1997.

Light Measurement using the Photometrics-PXL1300L CCD Camera

Sumanta N. Pattanaik* and Kenneth E. Torrance†

PCG-98-1 May 29, 1998

This report describes the spectroradiometric calibration of a CCD camera system, which consists of a high dynamic range (12 bit), liquid cooled scientific grade CCD camera used in conjunction with a series of narrow band and neutral density filters. The ultimate purpose of the calibration is to convert multiple single channel images obtained from the camera into a quantitative spectral image of a viewed scene. The present work extends earlier work [PCG-96-1] in which spectral transmittance curves for the filters and camera lens system were measured, and linearity tests of the CCD sensor output as a function of incident illumination strength, and camera shutter and lens aperture opening, were carried out. The present study specifically extends the prior report to include the effects of focal distance and the spectral response function of the camera. The report provides a comprehensive radiometric model for the camera and describes a method of spectral recreation from camera measurements. The present report also describes and demonstrates a method for converting camera measurements into quantitative colorimetric information in terms of XYZ-CIE matching functions.

*Research Associate, Program of Computer Graphics, Cornell University.
†Professor, Sibley School of Mechanical and Aerospace Engineering, Cornell University.